Journal of Materials Chemistry C

ROYAL SOCIETY OF CHEMISTRY

COMMUNICATION

View Article Online
View Journal | View Issue

Cite this: J. Mater. Chem. C, 2023, 11, 4328

Received 2nd November 2022,
Accepted 20th February 2023

DOI: 10.1039/d2tc04659h

rsc.li/materials-c

An insight into the temperature dependence of photoluminescence of a highly-emissive Cs-Ag(Na)Bi(In)Cl_6 perovskite

Oleksandr Stroyuk, *[a] Oleksandra Raievska,[a] Andres Osvet,[b] Jens Hauch[ab] and Christoph J. Brabec[ab]

The temperature-dependent evolution of the photoluminescence (PL) properties of a highly emissive $Cs_2Ag_{0.35}Na_{0.65}Bi_{0.02}In_{0.98}Cl_6$ perovskite was examined in the range of 80–340 K. The PL maximum exhibited a shift to higher energies with an increase in *T*, while the bandgap decreased with elevated *T*. This behavior can be explained by a thermal distribution of the self-trapped exciton states.

Lead-free halide perovskites often reveal highly efficient broadband photoluminescence (PL) originating from self-trapped exciton (STE) states, which paves the way for numerous applications in "white" LEDs, light down-shifting materials for photovoltaics, luminescent sensors, *etc.*[1–6] The STE states form due to a strong electron–phonon interaction resulting in a high distortion of the sites of exciton localization and a large phonon contribution to the PL emission.[7,8] For this reason, the PL behavior of LFPs depends considerably both on the internal structure (composition, doping, vacancies, defects, *etc.*) and external stimuli (temperature, pressure), opening many opportunities for further studies of the mechanisms and dynamics of radiative STE recombination.

Recently we have reported a "green" synthesis procedure for highly stable $Cs_2Ag_xNa_{1-x}Bi_yIn_{1-y}Cl_6$ (CANBIC) perovskites emitting broadband yellow-white PL with the quantum yield (QY) reaching 92%.[9] In a follow-up report we provided a deeper insight into the factors affecting the PL QY of CANBIC compounds and further increased PL QY to 98%.[10] Here we track the evolution of the spectral properties of the highly-emissive CANBIC with $x = 0.35$ and $y = 0.02$ in a broad temperature range (80–340 K) by a combination of UV-Vis absorption, PL, and time-resolved PL spectroscopy. Using the concerted absorption and PL measurements we reveal a special temperature-dependent behavior of CANBIC perovskite.

The CANBIC perovskite was produced in open-air ambient conditions according to a previously reported protocol *via* a controlled interaction between metal cations and chloride anions in 2-propanol/water mixtures.[9] The purified CANBIC was redispersed in 2-propanol and drop-cast on a glass substrate for spectral studies (see photograph in Fig. 1a). The CANBIC sample contains 0.5–3 μm polygonal crystals with the perovskite *Fm3m* lattice,[9,10] showing a direct room-temperature (RT) bandgap of *ca.* 3 eV (Fig. 1a) and a broadband "yellow-white" PL emission band peaked at 2.2 eV at RT (Fig. 1b).

The CANBIC sample was placed into a thermostat, cooled to 80 K, and then UV-Vis reflectance and PL spectra were taken simultaneously with the temperature increasing up to 340 K in intervals of 5–10 K. This series was reproduced for three separately prepared CANBIC samples. In addition to stationary PL measurements, we collected a series of PL decay curves at different temperatures.

Temperature elevation resulted in a gradual shift of the absorption edge of the CANBIC perovskite to lower energies as well as in a slight "red" shift and broadening of the

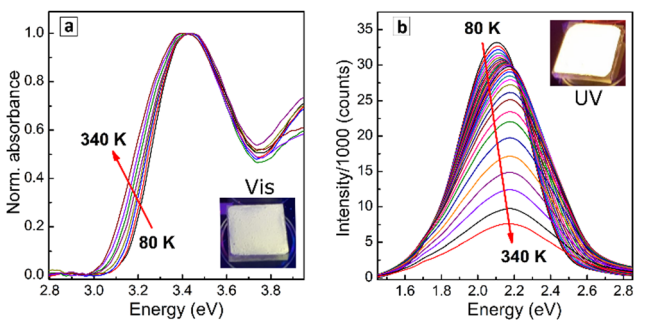

Fig. 1 Normalized absorption spectra (a) and PL spectra (b) of CANBIC perovskite at different temperatures. (a) Absorption spectra registered at 80, 140, 180, 210, 230, 260, 300, and 340 K (from left to right). (b) PL spectra registered from 80 K to 340 K with an incremental step of 5 K. Inset: Photographs of a CANBIC sample under ambient illumination (in (a)) and under UV illumination (340–360 nm, in (b)).

[a] Forschungszentrum Jülich GmbH, Helmholtz-Institut Erlangen Nürnberg für Erneuerbare Energien (HI ERN), Erlangen 91058, Germany. E-mail: o.stroyuk@fz-juelich.de
[b] Friedrich-Alexander-Universität Erlangen-Nürnberg, Materials for Electronics and Energy Technology (i-MEET), Martensstrasse 7, Erlangen 91058, Germany

absorption peak at *ca.* 3.4 eV (Fig. 1a). An increase in temperature was also found to affect strongly the intensity and spectral parameters of the PL band. The integral PL intensity (I_{PL}) decreased strongly as the temperature was elevated from 80 to 340 K (Fig. 1b). Simultaneously, a strong broadening of the PL band was observed as well as a rather unexpected "blue" shift of the PL band maximum. At the same time, the shape of the PL spectrum did not show any considerable changes and can be fitted with a single Gaussian profile in all cases. These changes were reproducible and identical for three different CANBIC samples and could be repeated in a reverse experiment decreasing the temperature from 340 K down to 80 K. In a further discussion we will focus on the temperature dependences of several key parameters – I_{PL}, the spectral width of the PL band (FWHM), bandgap, PL band maximum energy, and Stokes shift.

The integral PL intensity I_{PL} shows a rather sharp drop when the temperature is elevated from RT (290 K) to 350 K (Fig. 2a). At temperatures below RT, I_{PL} slightly increased with lowering T until it saturated at 220–250 K. At $T < 220$ K, a decrease of I_{PL} is observed with decreasing temperature coming to a second saturation state at 80 K $< T <$ 120 K (Fig. 2a).

Such behavior is typical for STE emission and is accounted for by the existence of a potential barrier E_b between the free-exciton and STE states. The section of the $I_{PL}(T)$ dependence at $T > 220$ K was fitted using the well-known expression[11–14]

$$I(T) = \frac{I_0}{1 + \text{const} \times \exp(-E_b/k_b T)}$$

where I_0 is I_{PL} at $T = 0$, and k_b is the Boltzmann constant. The potential barrier was estimated from the fit as E_b = 275 ± 5 meV (inset in Fig. 2a). Similar values were reported also for other compositions, such as CABIC (185 meV[12] and 186 meV[11]) and CAIC (*ca.* 250 meV[15]), indicating a general character of the STE states in these materials.

The FWHM of the PL band was found to increase by a factor of almost two with the temperature elevated from 80 to 340 K (Fig. 2b). This thermal evolution of the PL FWHM is related to the Huang-Rhys factor S and phonon energy E_{ph} as[13,16,17]

$$\text{FWHM}(T) = 2.36\sqrt{S}E_{ph}\sqrt{\coth\left(\frac{E_{ph}}{2k_b T}\right)}$$

Fitting of the FWHM(T) dependence yielded an S value of 20 ± 1 and E_{ph} of 37 ± 2 meV (Fig. 2b). The large S value indicates a strong electron-phonon coupling in CANBIC perovskite responsible for the large Stokes shift and FWHM of the PL band. The E_{ph} value is very close to the LO (longitudinal optical) phonon mode observed in the Raman spectra of the CANBIC perovskite (300 cm^{-1}, 34 meV).[9,10]

The PL maximum energy grows with increasing temperature from *ca.* 2.10 eV at 80 K up to *ca.* 2.17 eV at 250–270 K, reaching saturation at higher T (Fig. 2c, curve 2). This behavior is opposed to the typical behavior of semiconductor materials which show a shift in PL maximum to lower energies with increasing T.

Such unusual behavior was also reported for several perovskite systems, including $CsPbBr_3$,[18] $CsSnI_3$,[19] $Cs_2Ag_xNa_{1-x}BiCl_6$,[20] and Cs_2MBiI_6, M = Na and K,[14] and explained by a combination of structural and electronic factors changing with temperature in different directions. We note, however, that in the reports discussing the unusual T-dependent shift of the PL maximum, the bandgap E_g of the tested material was deduced mostly from the position of the PL maximum with no independent bandgap measurements (absorption/reflectance or PL excitation spectra) provided for the same T range.[14,18,19] In the present case, we performed simultaneous measurements of PL and reflectance spectra of CANBIC perovskite at different T and calculated the bandgap values independently from the absorption band edge position.

Remarkably, the PL maximum and the bandgap were found to follow opposite trends with varied T. While the E_g decreases in an expected monotonous way with increasing temperature (Fig. 2c, curve 1), the PL maximum energy becomes higher (curve 2), thus showing a distinct temperature dependence of the Stokes shift (Fig. 2d). These results indicate that the bandgap of CANBIC perovskite shows a "normal" behavior which is expected from an excitonic transition in a semiconductor,[21] while the evolution of the PL maximum

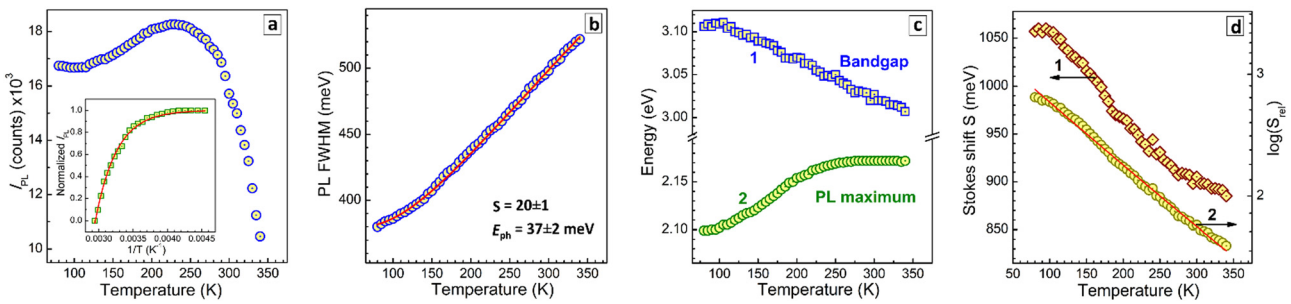

Fig. 2 Temperature dependence of the integral PL intensity I_{PL} (a), PL FWHM (b), bandgap (c, curve 1), PL maximum energy (c, curve 2), and Stokes shift S (scatter 1 in d). Scatter 2 shows relative Stokes shift S_{rel} as a function of T, and the solid line represents fitting of the experimental dataset 2 with an exponential function. Inset in (a): a section of T-dependence of PL intensity in coordinates $I_{PL}^{-1} - T^{-1}$. Solid lines in (a), (b), and (d) represent the results of the fitting.

position is not related directly to the bandgap change but reflects the independent evolution of the character of the emitting state.

Tracking the change in the Stokes shift with temperature allows the effect of lattice expansion to be excluded and the thermal evolution of the relaxation of the excited state to be exclusively followed. In the case of "classic" semiconductors with excitonic PL emission, the Stokes shift shows no changes[22] or a small decrease[23,24] in a broad T range (typically above 50 K).

For lead-based halide perovskites, such as $CsPbBr_3$ and $MAPbBr_3$, a considerable increase of the Stokes shift with increasing temperature was reported[25] and interpreted as a result of stronger carrier-lattice interactions at higher temperatures, unique for this type of semiconductor.

The special temperature dependence of the Stokes shift reported here was also observed for other lead-based and lead-free perovskites,[14,18–20] all having the self-trapped excitonic character of the excited state. It should be noted that the strongly localized character of the STE states in the halide perovskites makes them very similar to molecular systems, where a high degree of localization of the excitation energy is expected, in particular, to J-aggregates of dyes[26] and to organic excimers.[27]

In the particular case of radiative relaxation in J-aggregates, a simple model of the totally accessible density of states (DOS) was proposed to interpret the temperature dependence of the spectral parameters of the fluorescence band (peak position, spectral width).[26] This model assumes the PL spectrum $F(h\nu)$ to be a product of the low-temperature (T = 0) absorption spectrum $A(h\nu)$ and an exponential function describing the thermal distribution of possible excitonic states, $F(h\nu) = A(h\nu) \times \exp(-h\nu/k_BT)$, where $h\nu$ is the energy, and k_B is the Boltzmann constant.

The temperature dependence of the Stokes shift S of CANBIC perovskite reported here was found to be well described by the above model. The logarithm of relative Stokes shift, S_{rel}, expressed in the units of PL bandwidth w as $S_{rel}(T) = S(T)/w(T)$, was found to increase in a linear manner as the temperature decreased (Fig. 2d, scatter 2). The $S_{rel}(T)$ dependence can be fitted with a function $S_{rel} = a \times \exp(-T/b)$,[26] with the best-fit parameters a = 3.16 and b = 433 K or 37 meV (Fig. 2d, solid line), indicating an exponential temperature dependence of the Stokes shift, in accordance with the totally accessible DOS model.[26] The parameter b is very close to the energy of LO phonon in CANBIC perovskite,[9,10] additionally indicating a strong interaction between the photoexcited charge carriers and the perovskite lattice.

The model of totally accessible DOS provides a natural explanation for the observed peculiar temperature dependences of the PL parameters, particularly for the "red" shift of the PL band maximum and the growth of the Stokes shift at decreasing temperatures. The applicability of this model can be taken as an indication that the STE states photogenerated in CANBIC perovskites behave more like excited states in molecular crystals than the excitons in classic semiconductors.

The PL decay of CANBIC is considerably accelerated by elevating T from 80 K to 340 K (Fig. 3a). At all temperatures,

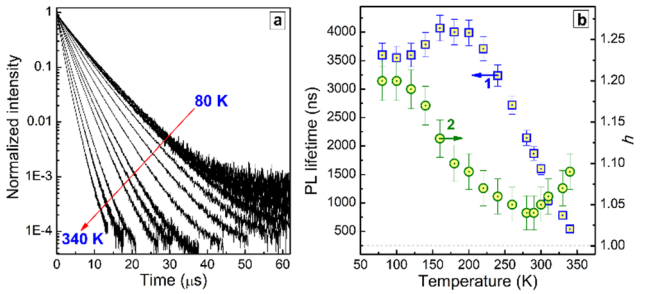

Fig. 3 (a) PL decay curves detected for CANBIC perovskite at different T from 80 K to 340 K. (b) PL lifetime τ (1) and heterogeneity parameter h (2).

the PL decay curves showed a certain deviation from single-exponential character. To simultaneously extract the PL lifetime and to quantitatively evaluate the deviation from the single-exponential decay, the PL transients were fitted with a stretched-exponential function[21–23]

$$I(T) = I_0 \exp\left(-\frac{t}{\tau}\right)^{\frac{1}{h}}$$

The fits provide a PL lifetime τ and a heterogeneity parameter h, which is equal to unity for single-exponential decay and larger than 1 for more complex curve shapes.

In the context of the radiative recombination in solids, the heterogeneity parameter is often regarded as a measure of random fluctuations of the lattice or a local defect close to the recombination site resulting in a variation of the emission lifetime even for a single emitting state.[22,23] For the case of broad-band-emitting CANBIC perovskites, the heterogeneity parameter can be related to the above-discussed temperature-dependent distribution of possible energies of the STE state.

The fitting of the T-dependent PL decay curves of CANBIC perovskite showed that the PL lifetime is similar to the temperature dependence of PL intensity I_{PL}, strongly increasing from a few hundred ns at 340 K to almost 4 μs at 200 K and then slightly decreasing to *ca.* 3.5 μs at T < 150 K (Fig. 3b, scatter 1).

The heterogeneity parameter shows a moderate decrease down to *ca.* 1.03 as T is lowered from 340 K to room temperature, but increases steadily at lower T reaching almost 1.2 at T < 100 K (Fig. 3b, scatter 2). In light of the above interpretation of non-exponential STE PL decay, the increase of h at lower T can be assigned to a change in the energy distribution of the STE states.

In conclusion, we examined the evolution of the PL properties of the highly luminescent CANBIC perovskite in a temperature range of 80–340 K tracking both spectral parameters of the PL band and time-resolved PL behavior. The PL lifetime showed a distinct temperature dependence increasing from *ca.* 0.5 μs at 340 K up to *ca.* 4 μs at 160–200 K. The position of the PL maximum exhibited an unusual temperature dependence shifting to lower energies at lower temperatures, while the bandgap increased with a temperature decrease following the trend typical for semiconductor materials. These phenomena can be naturally explained by a model of the totally accessible density of states developed earlier for the molecular aggregates. This model assumes a thermal distribution of the energies of

possible STE states which is partially ''frozen out'' at lower temperatures resulting in a red shift and narrowing of the PL band as well as in the considerable growth of the Stokes shift.

Experimental methods

Reflectance spectra were recorded using a BlackComet spectrometer (StellarNet Inc.) and a 75 W Xenon lamp (Thorlabs) as an excitation source. The spectra were registered with an optical Y-fiber probe in identical geometry for the samples and reference (ultra-pure $BaSO_4$, Alfa-Aesar). Absorption spectra were then calculated by dividing the reflectance spectra of the lamp and the sample and subtracting the baseline. PL spectra were registered similarly to the reflectance spectra using a BlackComet spectrometer in the range of 190–1000 nm with a UV LED (365 nm, Thorlabs) as an excitation source. Temperature dependences of PL and reflectance spectra were collected using an Optistat DN-X cryostat (Oxford Instruments) controlled by a MercuryiTC temperature controller (Oxford Instruments) in the range of 80–340 K. The samples were drop-cast as suspensions in 2-propanol on glass and dried under ambient conditions. Photographs of luminescent CANBIC perovskites were taken at ambient conditions and under illumination with a UV lamp (350–370 nm). Kinetic curves of the PL decay were registered using a custom-designed setup based on a FluoTime300 luminescence spectrometer (Picoquant) equipped with a 402-nm LDH-P-C-405B laser. The excitation beam was guided to the samples by an optical fiber and the PL signal was collected in the range of 420–800 nm with excitation and emission slits set to 4 nm. In the case of *T*-dependent time-resolved PL measurements, the samples were placed in the Optistat DN-X cryostat, which was optically coupled with the spectrometer.

Author contributions

O. Stroyuk: conceptualization (lead), investigation (equal), writing – original draft preparation (lead); O. Raievska: investigation (lead), methodology (lead); A. Osvet: investigation (equal), writing – review & editing (equal); J. Hauch: conceptualization (equal), project administration (lead), writing – review & editing (equal); C.J. Brabec: conceptualization (equal), funding acquisition (lead), writing – review & editing (equal).

Conflicts of interest

There are no conflicts to declare.

Acknowledgements

The authors gratefully acknowledge the financial support of The German Federal Ministry for Economic Affairs and Climate Action (project Pero4PV, FKZ: 03EE1092A) and The Bavarian State Government (project ''ELF-PV-Design and development of solution-processed functional materials for the next generations of PV technologies'', No. 44-6521a/20/4). CB and AO gratefully acknowledge financial support by the Deutsche Forschungsgemeinschaft under GRK2495/E.

Notes and references

1 H. Tang, Y. Xu, X. Hu, Q. Hu, T. Chen, W. Jiang, L. Wang and W. Jiang, *Adv. Sci.*, 2021, **8**, 2004118.
2 N. K. Tailor, S. Kar, P. Mishra, A. These, C. Kupfer, H. Hu, M. Awais, M. Saidaminov, M. I. Dar, C. Brabec and S. Satapathi, *ACS Mater. Lett.*, 2021, **3**, 1025–1080.
3 Y. Gao, Y. Pan, F. Zhou, G. Niu and C. Yan, *J. Mater. Chem. A*, 2021, **9**, 11931–11943.
4 P.-K. Kung, M.-H. Li, P.-Y. Lin, J.-Y. Jhang, M. Pantaler, D. C. Lupascu, G. Grancini and P. Chen, *Sol. RRL*, 2020, **4**, 1900306.
5 W. Ning and F. Gao, *Adv. Mater.*, 2019, **31**, 1900326.
6 X. Li, X. Gao, X. Zhang, X. Shen, M. Lu, J. Wu, Z. Shi, V. L. Colvin, J. Hu, X. Bai, W. W. Yu and Y. Zhang, *Adv. Sci.*, 2021, **8**, 2003334.
7 Z. Xu, X. Jiang, H. Cai, K. Chen, X. Yao and Y. Feng, *J. Phys. Chem. Lett.*, 2021, **12**, 10472–10478.
8 S. Li, J. Luo, J. Liu and J. Tang, *J. Phys. Chem. Lett.*, 2019, **10**, 1999–2007.
9 O. Stroyuk, O. Raievska, A. Barabash, M. Batentschuk, A. Osvet, S. Fiedler, U. Resch-Genger, J. Hauch and C. J. Brabec, *J. Mater. Chem. C*, 2022, **10**, 9938–9944.
10 O. Stroyuk, O. Raievska, A. Barabash, C. Kupfer, A. Osvet, V. Dzhagan, D. R. T. Zahn, J. Hauch and C. J. Brabec, *Mater. Adv.*, 2022, **3**, 7894–7903.
11 S. Li, H. Wang, P. Yang, L. Wang, X. Cheng and K. Yang, *J. Alloys Compd.*, 2021, **854**, 1–8.
12 K. Dave, W. T. Huang, T. Leśniewski, A. Lazarowska, D. Jankowski, S. Mahlik and R. S. Liu, *Dalton Trans.*, 2022, **51**, 2026–2032.
13 K. M. McCall, C. C. Stoumpos, S. S. Kostina, M. G. Kanatzidis and B. W. Wessels, *Chem. Mater.*, 2017, **29**, 4129–4145.
14 A. Singh, P. Dey, A. Kumari, M. K. Sikdar, P. K. Sahoo, R. Das and T. Maiti, *Phys. Chem. Chem. Phys.*, 2022, **24**, 4065–4076.
15 J. Luo, X. Wang, S. Li, J. Liu, Y. Guo, G. Niu, L. Yao, Y. Fu, L. Gao, Q. Dong, C. Zhao, M. Leng, F. Ma, W. Liang, L. Wang, S. Jin, J. Han, L. Zhang, J. Etheridge, J. Wang, Y. Yan, E. H. Sargent and J. Tang, *Nature*, 2018, **563**, 541–545.
16 Q. Hu, G. Niu, Z. Zheng, S. Li, Y. Zhang, H. Song, T. Zhai and J. Tang, *Small*, 2019, **15**, 1903496.
17 H. Siddique, Z. Xu, X. Li, S. Saeed, W. Liang, X. Wang, C. Gao, R. Dai, Z. Wang and Z. Zhang, *J. Phys. Chem. Lett.*, 2020, **11**, 9572–9578.
18 X. Yuan, P. Jing, J. Li, M. Wei, J. Hua, J. Zhao, L. Tian and J. Li, *RSC Adv.*, 2016, **6**, 78311–78316.
19 C. Yu, Z. Chen, J. Wang, W. Pfenninger, N. Vockic, J. T. Kenney and K. Shum, *J. Appl. Phys.*, 2011, **110**, 063526.
20 B. Ke, R. Zeng, Z. Zhao, Q. Wei, X. Xue, K. Bai, C. Cai, W. Zhou, Z. Xia and B. Zou, *J. Phys. Chem. Lett.*, 2020, **11**, 340.
21 K. P. O'Donnell and X. Chen, *Appl. Phys. Lett.*, 1991, **58**, 2924–2926.
22 C. Sasaki, H. Naito, M. Iwata, H. Kudo, Y. Yamada, T. Taguchi, T. Jyouichi, H. Okagawa, K. Tadamoto and H. Tanaka, *J. Appl. Phys.*, 2023, **93**, 1642.
23 H. Murotani, K. Ikeda, T. Tsurumaru, R. Fujiwara, S. Kurai, H. Miyake, K. Hiramatsu and Y. Yamada, *Phys. Status Solidi B*, 2018, **255**, 1700374.

24 S. D. Baranovskii, R. Eichmann and P. Thomas, *Phys. Rev. B: Condens. Matter Mater. Phys.*, 1998, **58**, 13081.
25 Y. Guo, O. Yaffe, T. D. Hull, J. S. Owen, D. R. Reichman and L. E. Brus, *Nat. Commun.*, 2019, **10**, 1175.
26 I. G. Scheblykin, O. Yu Sliusarenko, L. S. Lepnev, A. G. Vitukhnovsky and M. Van der Auweraer, *J. Phys. Chem. B*, 2001, **105**, 4636.
27 S. Hammer, T. Linderl, K. Tvingstedt, W. Brütting and J. Pflaum, *Mater. Horiz.*, 2023, **10**, 221.

